Electronic structure, ordering effects, phase stability, and magnetism in $Fe_{1-x}Cr_x$ systems

E. G. Moroni
Institut Physique Experimentale, Université de Lausanne, CH-1015 Lausanne, Switzerland
and Institut Romand de Recherche Numérique en Physique des Matériaux, PHB-Ecublens, CH-1015 Lausanne, Switzerland

T. Jarlborg
Département de Physique de la Matière Condenseé, Université de Genève, CH-1211 Genève, Switzerland
(Received 8 April 1992)

The total energies and magnetic properties of ideally ordered bcc Fe-Cr compounds and random substitutional disordered bcc $Fe_{1-x}Cr_x$ alloys are calculated using spin-polarized, self-consistent linear-muffin-tin-orbital-based methods. Calculated total energies are almost degenerate for magnetic and nonmagnetic states in $FeCr_3$, which is favorable for the Invar effect. Comparison with the results for complete disorder and with the total energies of the pure elements, lead to the conclusion that disordered states in the form of clusters, are stable at most concentrations. The effect of order is also crucial for the FeCr composition, where the CsCl structure gives ferromagnetic Cr moments, in contrast to the antiferromagnetic configurations in most other cases.

I. INTRODUCTION

Iron and chromium are constituents of many important magnetic materials. As pure element the former is a strong ferromagnet (FM), the latter a weak noncommensurate antiferromagnet (AF) and both are in the bcc structure. Alloys composed of the two, contain many interesting magnetic systems, and the degree of local ordering seems to influence the properties. In recent years many experiments have pointed out the similarities between certain properties in Fe-Cr alloys and the better-known Invar anomalies in Fe-Ni Invar systems, despite the different (fcc and bcc) crystal structures. It was found that in the range of 75–95% of Cr the alloy has vanishing thermal expansion coefficients as an Invar alloy.[1] It is generally agreed that the Invar properties are due to the closeness of and interplay between magnetic (M) and nonmagnetic (NM) ground states. The Weiss model[2] assumes thermal excitations between two electronic configurations of iron atoms (the AF and FM) that have almost the same energy but different volumes. Band theory[3] confirmed that the total energies of NM and FM configurations are almost degenerate near the Invar composition in the FeNi system. The most extraordinary Invar feature is the vanishing thermal expansion coefficient α in a wide temperature range. It is believed that the magnetic contribution to α is negative and compensates for the normally positive α that is due to lattice vibrations. Also the bulk modulus shows anomalous behavior such as a hardening with increased temperature. The vivid variation of elastic properties with pressure, temperature, and magnetic field, is characteristic for several Invar systems.

The magnetic phase diagram in Fe-Cr is FM up to about 80% of Cr where the average moment decreases linearly as a function of Cr composition and is close to a Slater-Pauling curve.[4] The regions where the FM and AF regimes overlap have been studied by different techniques, but the magnetic behavior in this composition range is not completely clarified. Experimental determination of the extent of antiferromagnetism is reported in Ref. 5. This transition region (at around 80% of Cr) between FM and AF regimes is characterized by the collapse of the total magnetic moment and of the Curie temperature. In this region the anomalous behavior of the specific heat coincides with the Invar behavior.[6] Moreover, a large number of experimental works have pointed out that for the Fe-Cr system the local magnetic properties are not only concentration dependent but depend strongly on the environment and on the method of preparation.

The structural phase diagram of FeCr alloys has been studied extensively and shows a miscibility gap indicating a decomposition in nonhomogeneous Fe-rich and Cr-rich components at low temperature. For $440\,^{\circ}\mathrm{C} < T < 830\,^{\circ}\mathrm{C}$ in the equiatomic region there is formation of a nonferromagnetic σ phase with a unit cell of tetragonal symmetry, but there are no indications that this or other ordered structures are stable at lower temperature. A miscibility gap has been found experimentally at a temperature $T_c \sim 500\,^{\circ}\mathrm{C}$ (Refs. 7 and 8), and the coherent line has been calculated and analyzed below the solubility limit.[9] Heat treatment can influence the chemical arrangements of atoms and short-range order effects (due to clustering) seem to affect strongly the magnetic and structural properties.

Theoretically, several studies of the pure elements have been done using local-spin-density (LSD) electronic-structure calculations. The results can explain many experimental findings but also led to some famous pitfalls

of the present form of LSD approximation, namely, to the question of the most stable structure of Fe and to the stability of the AF structure in Cr.

For some compositions of bcc $Fe_{1-x}Cr_x$ alloys the electronic structure has been studied by coherent-potential approximation (CPA) calculations[10,11] and Cr impurities in Fe have been studied by the Green's-function method.[12] The calculations on the bcc Fe-based FM alloys of Hasegawa and Kanamori[10] furnished a basic understanding of the behavior of the density of states (DOS) as a function of composition within a simple single band model. Pair potentials up to the third neighbor and their variation with Cr impurity concentration have been calculated using a generalized perturbation method.[13]

In order to study the manifold of properties in the Fe-Cr system we analyze, in this work, the ground-state properties of hypothetical ordered and completely disordered systems in the whole concentration range. As a part of this we also study the Invar problems, such as instability between different magnetic states. The comparison between the electronic and ground-state properties of the two phases (ordered and disordered) will provide a better understanding of the complex structural properties. The electronic structures are calculated for pure elements and of several concentrations of the Fe-Cr system both as ordered compounds by supercell linear-muffin-tin-orbital (LMTO) calculations and as disordered alloys by an approximate LMTO method for random occupation of the lattice sites.

The organization of the remainder of the paper is as follows. In Sec. II we outline the methods of calculation for ordered and disordered structures. The ground-state properties of pure Fe, Cr, and Fe-Cr and the formation energies of the ordered systems are presented in Sec. III, together with a comparison between different calculations for the energy of the disordered alloy. Section IV presents results on the magnetic and electronic properties of Fe and Cr in the Fe-Cr system as a function of composition and pressure. Section V compares the electronic band structure for the ordered supercell and the disordered phases as a function of composition. In Sec. VI we conclude, giving a summary of our results. As will be shown, many results are consistent with experiments, while other results indicate that the degree of short-range order determines the magnetic properties.

II. METHOD OF CALCULATION

A. Ordered structures

The electronic structures for various supercells are calculated using the self-consistent LMTO method.[14,15] The LSD approximation of Refs. 16 and 17 for the exchange-correlation potential of electrons is used (except for a test case on pure Cr). The basis contains up to $l = 3$ terms in tails and three-center terms. Overlap corrections, relativistic terms except for spin-orbit coupling, and relaxed-core functions are all included. The density-of-state (DOS) functions are calculated using the tetrahedron integration method with about $500/N$ k-points, where N is the number of atoms per unit cell. The method of calculation is the same as has been used for other Invar systems.[18] The ground-state properties are obtained from total-energy calculations. For the spin-polarized case we do not calculate the total energy of the system for constrained values of the magnetic moment, but at each fixed lattice parameter we let the self-consistency develop freely to its energy minimum. The total energy of the non-magnetic (NM) and magnetic (M) states is minimized at each composition with respect to the lattice parameter. A least-squares fit of the Birch type[19] is used to obtain the total energy as a function of volume. The variation of the pressure and the bulk modulus with volume can be obtained using the following equations: $P(V) = (B_0/B_0')[(V_0/V)^{B_0'} - 1]$ and $B(V) = B_0(V_0/V)^{B_0'}$, where we have chosen the special case $B_0' = 4$ because we found that sensitive variations of B_0' do not much influence the stability of the predicted values for V_0 and B_0.

The calculated energies of ordered phases are used in the Connolly-Williams[20] (CW) method in order to describe disordered states via an expansion of total energies in volume-dependent many-body cluster interactions. Similarly to Ising-like models, the excess energies of each ordered configuration (α) can be written as a cluster expansion,[20]

$$\Delta E^{\alpha}(V) = \sum_{\gamma} \xi_{\gamma}^{\alpha} v_{\gamma}(V), \tag{1}$$

where $v_\gamma(V)$ are independent many-body-cluster interactions and ξ_γ^α are multisite correlation functions. These correlation functions are defined as

$$\xi_{\gamma} = \frac{1}{N_{\gamma}} \sum_{p_i} \sigma_{p_1}\sigma_{p_2}\cdots\sigma_{p_\gamma} \tag{2}$$

where σ_{p_i} takes the value $+1$ or -1 depending on the occupancy of site p, N_γ is the total number of γ-type clusters, and the sum is over all γ-type clusters in the lattice. The expansion is useful if it converges rapidly, i.e., if the potentials diminish rapidly with the complexity of the clusters. Here we consider for the bcc lattice a cluster expansion with an irregular tetrahedron as the maximum cluster size.[21,22] This cluster expansion requires the calculation of six stoichiometric high-symmetry compounds with the bcc, $B2$, $B32$, and $D0_3$ structure types. The maximum cluster is an irregular tetrahedron formed by four nearest-neighbor (NN) pairs and two next-nearest-neighbor (NNN) pairs. The subclusters are the empty ($n = 0$), the point ($n = 1$), an the NN pair ($n = 2$), the NNN pair ($n = 3$), the irregular triangle formed by two NN pairs, and one NNN pair ($n = 4$). For the tetrahedron approximation, the cluster interaction energies $v_\gamma(V)$ are obtained simply by inversion of Eq. (1) and are given by

$$v_{\gamma}(V) = \sum_{\alpha} (\xi_{\gamma}^{\alpha})^{-1} \Delta E^{\alpha}(V). \tag{3}$$

At equilibrium [i.e., at the volume that minimizes $\Delta E^\alpha(V)$ of Eq. (1)] the excess energy simply gives the formation enthalpy for each ordered structure ΔH^α.

The formation energies are of the order of a few mRy per atom, and their calculation require accurate self-consistent methods. Moreover, for each unit cell, we take care to use similar integration techniques and consistent minimization procedures in order to avoid errors due to different approaches or different potentials. As Connolly and Williams[20] have shown, for a random solid solution the pair and higher-order many-body correlation functions are expressed as products of the point correlations, and we have that $\xi_\gamma^{\rm dis} = (x_{\rm Fe} - x_{\rm Cr})^{n_\gamma}$, where n_γ is the number of sites in the γ cluster, and x_i (i=Fe,Cr) are the relative concentrations of Fe and Cr atoms. Defined similarly to Eq. (1), the excess energy for the disordered alloy is then given by

$$\Delta E_{\rm tot}^{\rm dis}(V) = \sum_{\gamma}^{\gamma_{\rm max}} v_\gamma(V)\xi_\gamma^{\rm dis}. \tag{4}$$

The heat of formation for a random solid solution at a given x is defined as the minimum values of Eq. (4) with respect to the volume. The ordering energy E_o of each compound is then calculated as the difference of the heat of formation for the ordered compound and the random solid solution at the same composition. The CW method have been applied to several semiconductor and noble-metal-based alloys in order to study the temperature-composition phase diagram. Moreover, the role of chemical (volume- and composition-independent) and volume-dependent elastic interactions on the phase diagrams have been studied separately.[23] A generalization of the CW method to free energies containing vibrational entropies has been recently presented,[24] but more developments are necessary in order to produce accurate phase diagrams.

B. Substitutional disordered systems

For calculating the electronic structure for substitutionally disordered systems we have developed a simple method that is based on the standard LMTO technique. The basic idea is to calculate the local electronic structure (LES) for one pure site A, which is surrounded by an effective medium that is a concentration average over all sites. The Bloch sum of energy-independent muffin-tin orbitals may be written as a one-center expansion

$$\chi_L^k(r) = \phi_L(-l-1,r) - \sum_{L'} S_{L,L'}^k \phi_{L'}(l',r)\, \tilde{f}_{l'}, \tag{5}$$

where the usual notations are used.[14,15] The function $\tilde{f}$ depends normally on the potential of each site in the ordered lattice. In the case of disorder $\tilde{f}_l$ is averaged over all sites so that $\tilde{f}_l = c_A f_l^A + c_B f_l^B + \cdots$, where the sum of all concentrations $c_A + c_B + \cdots = 1$. The structure constant S^k is unchanged, since the lattice is the same with or without disorder, as long as the Wigner-Seitz radius is chosen to be the same for all sites. The function $\tilde{f}$ contains combinations of $R_l(-l-1)/\tilde{R}_l(-l-1)$ and $R_l(l)/\tilde{R}_l(l)$ and make the "tail" part of the band problem an "effective medium property." Here $R_l(D)$ is the amplitude of the l-radial wave function at the Wigner-Seitz (WS) sphere S evaluated at the energy for which the logarithmic derivative is D. $\tilde{R}_l(D)$ is the corresponding property for a concentration averaged wave function. The approximations lead to an assumption of complete disorder, i.e., one atom is surrounded by sites that have averaged scattering properties. This means that no effects of clustering or shell structures are taken into account. The charge density has the contribution from its own site and a tail contribution from the outside.[14,15] In the present case with disorder, this implies that a pure A (or $B\ldots$) site receives tails from the "averaged" site. Disorder modifies the normal band structure both in the eigenvalue problem via the new two- and three-center terms that enter from Eq. (5), and in the tail decompositions of the wave function into one-center expansions. This is repeated for the local electronic structure of A and B sites. In the present method (contrary to the CPA method) we introduce lifetime effects or band-broadening effects in a second step as a perturbation, so that a broadening parameter $\Delta\epsilon$ with the dimension of energy is calculated due to the fluctuation of the potential in the tail region:

$$\Delta\epsilon_A^k = \sum_{q\neq A,l} n_{q,l}^k 4\pi \int r^2 |R_{q,l}(E_A,r)|^2 \Delta V(r) d^3r. \tag{6}$$

Here the sum over q is over the sites other than the one at the origin, R is the radial wave function, n_{ql} is the local character, and $\Delta V(r)$ is the difference of the local potential compared to the average potential. The parameter $\Delta\epsilon$ is used in a Gaussian broadening function of each band. An additional thermal broadening of 5 mRy is used for all the studied cases. Other aspects of the electronic structure method are the same as in our LMTO method for ordered periodic lattices.[15] Self-consistency, including relativistic core states, are carried out; f states are included as well as the combined correction term for the sphere overlap. The Madelung energy is calculated using a nonoverlaping sphere geometry.[15]

The method leads to very simple and rapid calculations. If the alloy contains N number of constituents one needs only to perform N LMTO band calculations, each one as with one atom per unit cell. The Fermi energy is determined by filling the sum of partial DOS functions with the number of available electrons. This is done at each iteration until convergence. The scaling properties of the band problem is therefore very advantageous compared to the supercell approach. Instead for LMTO matrices of rank $M9$ (M atoms per unit cell) the averaged-band problem considers matrices of rank 9 solved N times. The present method has been tested and applied to various alloy systems. Calculated DOS functions for $Cu_{1-x}Ni_x$ (Ref. 25) and $Ag_{1-x}Pd_x$ compare very well with photoemission measurements[26] and CPA calculations.[27] In the studies of the $Fe_{1-x}Cr_x$ systems we will compare with the results of the supercell calculations, which are restricted to x=0, 0.25, 0.50, 0.75, and 1.0. Here the advantage is that identical procedures have been employed as much as possible in the two approaches, and total energies and

TABLE I. Comparison between equilibrium values of lattice constant, bulk moduli, and magnetic moment for bcc Fe and Cr calculated using LSD and PW approximation by different methods. VWN stands for LSD Vosko, Wilk, and Nusair parametrization (Ref. 52), GL and vBH for the Gunnarsons-Lunqvist and von Barth–Hedin LSD form (Refs. 16 and 53), and PW for the Perdew-Wang gradient-corrected LSD functional.

Element	Method		a(a.u.)	B (Mbar)	M (μ_B)
	LMTO (1 atom/cell, $l = 3$)	VWN	5.25	2.30	2.26
	LMTO (2 atoms/cell, $l = 2$)	GL	5.29	2.36	2.15
	LAPW [a]	VWN	5.21	2.66	2.08
Fe	FLAPW [b]	VWN	5.21	2.72	2.18
	FLAPW [b]	vBH	5.24	2.29	2.07
	LMTO [c]	PW	5.47	1.70	2.30
	FLAPW [d]	PW	5.44	1.82	2.127
	Expt.		5.40	1.72	2.12
	LMTO (2 atoms/cell, $l = 2$)	GL	5.36	2.51	0.00
	LMTO (2 atoms/cell, $l = 2$)	PW	5.56	1.46	1.20
	LAPW [e]	VWN	5.28	2.65	0.70
Cr	LAPW [e]	vBH	5.27	2.86	0.67
	APW [f]	vBH	5.38	2.54	0.00
	Expt.		5.44	1.90	0.59

[a]Reference 32.
[b]Reference 54.
[c]Reference 28.
[d]Reference 55.
[e]Reference 38.
[f]Reference 39.

other sensitive quantities can be compared. However, in the interpretation of the results it has to be remembered that the disorder calculations refer to the limit of extreme disorder, in which no clusters appear.

III. GROUND-STATE PROPERTIES AND HEAT OF FORMATION OF Fe-Cr COMPOUNDS

A. Pure Fe and Cr

For pure Fe and Cr several LSD calculations using different methods are avalaible, and we compare our calculations with previous results obtained by other works in Table I. We find that different methods, different functional forms of the exchange-correlation potential, different numbers of atoms per unit cell, different choices of basis (if f states are included or not), and the type of constraint imposed [i.e., if the fixed-spin-moment (FSM) technique is used] can give slightly different results. For iron, LSD predicts a NM fcc ground-state instead of a FM bcc, and for bcc Cr we find (using the CsCl structure with two atoms per cell and without FSM) that at equilibrium the NM and AF states coexist (see Table II and Fig. 1). The total-energy difference between the M and NM phase for these systems is a delicate quantity to calculate and different methods give different values. For iron the energy difference between the minima of FM-bcc and NM-fcc total energies found by many authors[28,31,32] varies from 2 to 6 mRyd/atom. In the LSD approximation the cohesive energy for bcc iron is found to be $E_{\rm coh} = -0.48$ Ry and is higher than the experimental value $E_{\rm coh} = -0.32$ Ry. For $3d$ transition metals Bagno, Jepsen, and Gunnarsson[33] have shown that gradient corrections [in particular the Perdew-Wang[34,35] (PW) version] improve the total energies. Subsequent works[28] (see Table I) have shown that the PW potential leads to an

TABLE II. Calculated ground-state properties of FM- and NM-ordered Fe-Cr compounds. ΔE are the total-energy differences per atom between the NM and FM minima, and ΔH are the enthalpies of formation for FM Fe-Cr compounds.

Composition	Structure	$a_{\rm NM}$ (a.u.)	$a_{\rm FM}$ (a.u.)	$B_{\rm NM}$ (Mbar)	$B_{\rm FM}$ (Mbar)	ΔE (mRy)	ΔH (mRy)
Fe_2	$B2$	5.18	5.29	3.00	2.36	22.7	0.0
Fe_3Cr	$D0_3$	5.23	5.29	3.15	2.33	13.4	2.13
FeCr	$B2$	5.28	5.30	2.46	2.69	4.1	11.62
FeCr	$B32$	5.27	5.31	2.88	2.66	7.5	3.4
$FeCr_3$	$D0_3$	5.32	5.34	2.76	2.57	0.7	6.06
Cr_2	$B2$	5.36	5.36	2.83	2.51	−0.2	0.0

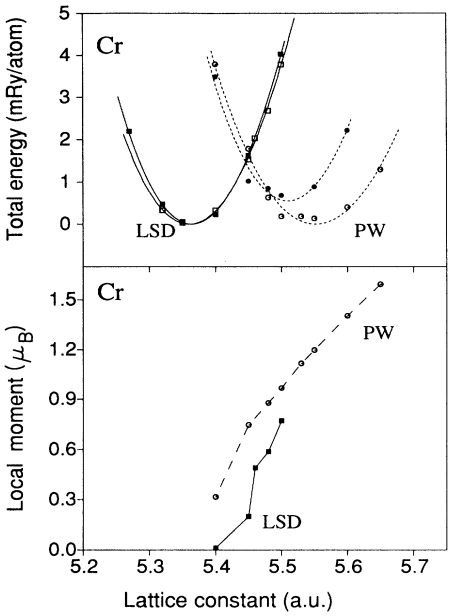

FIG. 1. Total energy and local magnetic moment as a function of lattice parameter for bcc Cr. The solid lines are calculated using LSD approximation, while the dashed lines are calculated using the Perdew-Wang gradient-corrections to LSD. The total-energy curves are displaced in energy so that the AF coincides.

overestimation of the lattice constants and compressibilities in $4d$ and $5d$ transition metals (TM's). Moreover, using the PW potential, even if we obtain the right ground state for iron, the computed structural energy difference between the bcc FM and fcc NM phase is of about 14 mRy, and is three times larger than the experimental results.[29]

In pure Cr different calculations give sometimes qualitatively different results, since there is a delicate balance between NM and AF configurations. We find almost degenerate AF and NM states, but with the balance slightly turned to the nonmagnetic state when LSDA is used. Kubler[36] found also near degenerate states but with the AF state lowest. Skriver[37] obtained an AF configuration, but did not compare total energies. Chen, Singh, and Krakauer[38] found the AF configuration stable over the NM configuration with about 4 mRy/atom, while Moruzzi and Marcus[39] report a FSM calculation, where the NM configuration is stable over the AF configuration (which is present only at large volume) with about 4 mRy/atom. Moreover, they indicate that a correct separation of the NM and AF states, using FSM, can improve the equilibrium properties in Cr. All these results are based on the assumption of a commensurate AF spin state, contrary to the real near commensurate spin wave in Cr.[40] The scattered results using different methods and potentials lead to the conclusion that total-energy differences smaller than about 1 mRy/atom are too small for a quantitative description of the physical properties.

As shown in Fig. 1, our calculated total-energy difference between the AF and NM states (in the two-atom CsCl-type unit cell) is lower than ~ 1 mRy at various lattice constants. For the AF curve the derived bulk modulus is about 30% higher than the experimental value, and we find a cohesive energy of $E_{\rm coh} = -0.382$ Ry while the experimental value is $E_{\rm coh} = -0.301$ Ry.[40] In Fig. 1 are shown also the calculated total energy and local moment on Cr using PW functional for the exhange-correlation potential. The calculated equilibrium properties are given in Table I. Analogously to the FM pure elements (Fe,Co,Ni), gradient correction to LSD stabilizes the magnetic phases of Cr with respect to the NM pure elements, increasing the local moments on Cr_2 and shifting the lattice minimum to higher values. However, gradient corrections take away the near degeneracy of NM and AF states in Invar systems.[41] Here for Cr, the PW functional fails in predicting the local magnetic moment that is found to be larger than the experimental result, and the theoretical lattice constant is also larger than the experimental one. Similar results have been found recently for Cr (Ref. 30) using a full-potential method. These systems seem to be good candidates for testing new potentials because of the required closeness of NM and M states.

B. Total energies and Invar systems

For the bcc lattice we have calculated the electronic structure of the NM and M phases for the ordered Fe_2,Cr_2, and FeCr with the $B2$ and the $B32$ structure and $FeCr_3$ and Fe_3Cr with the $D0_3$ structure. The latter structure has three inequivalent sites, and the lattice is of high symmetry and has a Brillouin zone of a fcc lattice. For each type of structure the atoms of Fe and Cr are chosen to have the same muffin-tin radius. The equilibrium lattice constants and bulk moduli of the NM and M states and the separation of total energy (in mRy/atom) of the calculated minima for each ordered phases are listed in Table II. The total energies of the NM and M phases are shown in Fig. 2 for the five compositions as a function of the lattice parameter. At each composition the magnetic state is the equilibrium state, and in good agreement with experiment our calculation predicts an increase of the lattice parameter as a function of Cr content. The difference in total energy between the calculated NM and M phases decreases monotonically with Cr composition and becomes almost zero in the Cr-rich region (see Table II). Experimental analysis of the temperature dependence of the saturation magnetization and thermal expansion of $Fe_{1-x}Cr_x$ has revealed anomalies similar to Invar type material in the range of x between $0.75-0.94$.[1] These experiments show that Invar anomalies are not only bound to a fixed structure (fcc) but can be present in other structures with different types of magnetic order.[42]

Our total-energy results confirm the possible Invar behavior of ordered Cr-rich systems, since we find nearly degenerate M and NM states for $FeCr_3$ and pure Cr. The differences in equilibrium volumes decrease as x goes to one. This difference is too small to give an Invar effect in Cr_2, while for $FeCr_3$ the conditions are similar but per-

haps less evident than in the fcc Fe_3Ni system.[18] Invar properties that are calculated in the two-state model[18] vary sensitively with the exact shape of the total-energy curves of the M and NM states, and this fact makes a quantitative determination uncertain. However, qualitatively the conditions for Invar behavior are clearly identified. For the bcc structure we find the Invar composition (at which the total-energy separation is small, but with a separation of volumes[18]) around 6.5 e/atom, differently from fcc Invars where the Invar anomalies are observed at around 8.5 e/atom for FM alloys[43] and 7.5 e/atoms for AF alloys.[44–46] The iron-rich alloy Fe_3Cr is found to be FM stable with a larger energy separation between NM and M states ΔE than in FeCr. For FeCr we studied the $B2$ and $B32$ structure and find that the equilibrium and magnetic properties of the two phases differ quite substantially; the obtained energy difference between the two structures of the same composition is 8 mRy/atom and 9.4 mRy/atom, for FM and NM phases, respectively. This suggests an instability of the most ordered $B2$ structure. Moreover, the total energies of NM $B2$ FeCr are difficult to stabilize because the Fermi level is positioned in the middle of a large peak of the density of states (DOS) (see Fig. 6).

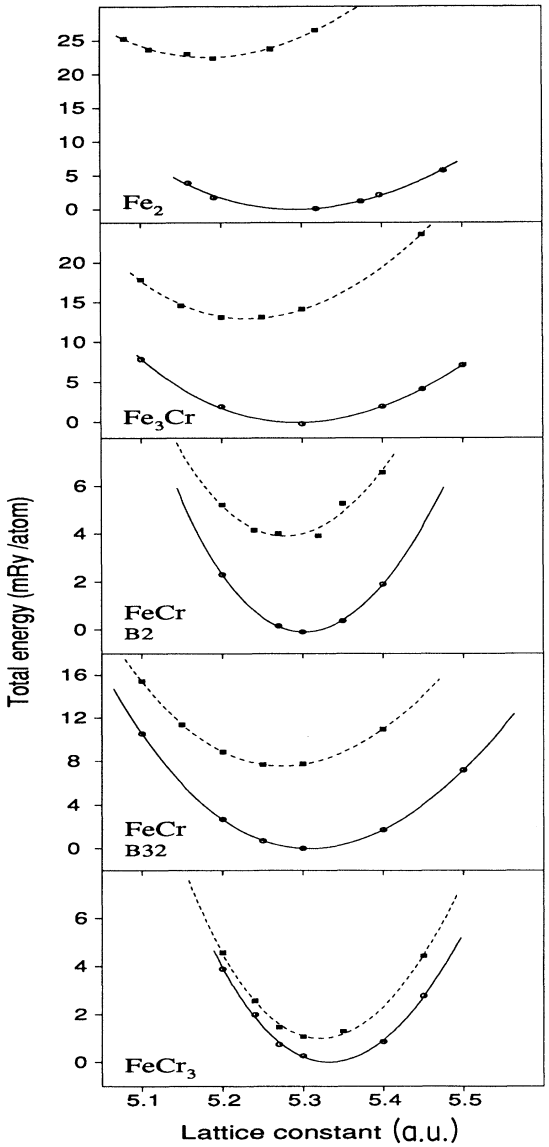

FIG. 2. Calculated total energies vs lattice constant of the NM (dashed line) and M (solid line) phases for ordered bcc Fe_2, Fe_3Cr, FeCr, and $FeCr_3$ compounds. In the bcc lattice the $B2$ and the $B32$ structure type have been considered for FeCr, while $FeCr_3$ and Fe_3Cr retain the $D0_3$ type structure. The solid and dashed lines are Birch equations of state fitted to the calculated points.

C. Energies of formation and cluster interactions

In Table II are shown the calculated formation energies for all the studied FM Fe-Cr compounds. The stoichiometric compounds are metastable with positive energies of formation in agreement with experimental findings for which no ordered structures are found at low temperature. Ferromagnetism affects strongly not only the equilibrium properties of the system but also the calculated heat of formation stabilizing the magnetic phase in the Fe-rich part, and shifting to higher total energy the $B2$ phase with respect to the $B32$ for the equiatomic compositions. As described in Sec. II, we compute from Eq. (3) the volume-dependent many-body interactions potentials for the NM and FM alloys using a tetrahedron cluster expansion. Our results indicate poor convergence for the tetrahedron cluster expansion because the interaction V_5, associated with the irregular triangle, is of the same order of the NN-pair interaction; moreover V_5 shows quite high dispersion, while all the other higher-order cluster interactions vary slowly as a function of volume. The pair interactions V_3, V_4, and the tetrahedron interactions V_6, are $-5.8, 1.2, 0.3$ (mRy/atom), respectively. For the paramagnetic alloys the value of V_3, V_4, and V_6 are, respectively, $-1.3, 1.7$, and 0.5 mRy/atom and do not change with lattice parameter, while V_5 vary from 0.8 to -2 mRy/atom when the lattice changes from 5.29 to 5.36 a.u. These results indicate that for NM Fe-Cr system it is necessary to go beyond the tetrahedron cluster expansion. Aware of these limitations we present here only a restricted study.

The enthalpy of the NM and M phases of the ordered Fe-Cr compounds are shown in Fig. 3. The calculated energies of formation for the disordered random alloys are positive. This means that the alloys are most stable as clusters of pure Fe and Cr. The pure elements have different lattice constants at equilibrium, which implies that there should be internal strains within rather large clusters to relax the local volume within each cluster to its equilibrium value. Or, if the clusters are small, the local relaxation is not possible and the lattice constant is the same everywhere. The enthalpy calculated at the same averaged lattice constant is only 1–2 mRy higher than in the former case. However, the energy due to cluster boundaries should be added. This has not been calculated and it cannot be concluded if the clusters are large or small. On the other hand it is noted that the dif-

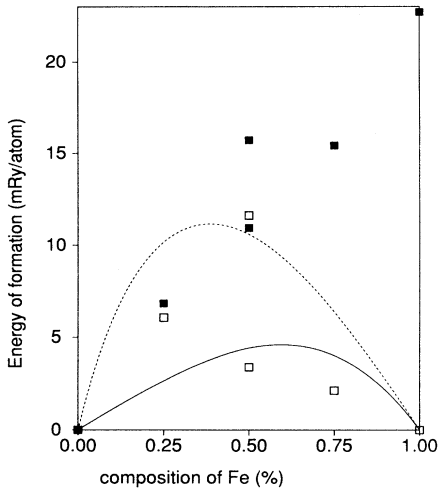

FIG. 3. Enthalpy of formation as a function of iron composition for Fe-Cr system at zero temperature. The energy of formation for a random solution for FM alloys (solid line) and NM alloys (dashed line) obtained using the tetrahedron cluster expansion, are compared to the energies of the FM ordered compounds (open boxes) and to the NM (solid boxes) ordered compounds. We consider as zero-energy reference the ground-state of pure Fe and Cr.

ference energy between M and NM states for a structure of clusters, is too large to explain the Invar effect in the $Fe_{0.2}Cr_{0.8}$ concentration range. Therefore, at this concentration it can be concluded that large clusters (where the energies due to boundaries is negligible) are unlikely. These findings are in fair agreement with experiments, since a miscibility gap has been found in the FeCr system. In reality it seems that the clusters do not consist of absolutely pure Fe or Cr, but contains some fraction of the other element. In the temperature range 500–800 K, corresponding to about 4 mRy, miscibility is found. This is smaller but still of the correct magnitude as our calculated values of about 5 mRy at 50-50 composition for M disordered alloys and 10 mRy for NM disordered alloys. The calculated variation of the lattice constant with composition for the disordered NM and FM $Fe_{1-x}Cr_x$ does not follow a Vegard rule. The calculated lattice constant are shifted above the Vegard lattice in the iron rich region (60–100 % Fe) and below it in the Cr-rich region.

IV. MAGNETIC AND ELECTRONIC PROPERTIES

A. Magnetic moments and hyperfine interactions

In 3*d* transition metals and alloys the knowledge of the magnitude of the local moments and their pressure dependence is important because they are directly related to the bulk properties of the materials. The Fe magnetism in the bcc structure is more stable (i.e., depends less on volume and electronic concentration variations) than in fcc structure. In Fig. 4 are shown the calculated local moments at different lattice constants and for different compositions. These calculations show that for the ordered phases the effects due to volume variations are less important than the effects due to variations of coordination number. In agreement with the magnetic phase diagram we find that bcc Fe_xCr_{1-x} is FM up to about 75% of Cr. As a function of volume we do not observe magnetic transition in the ordered system and no AF ordering is found in bcc Fe_xCr_{1-x} on the Fe site, while the noncontinuous variations of the Cr moment as a function of composition is quite remarkable. For Fe_3Cr one Fe atom retains the same value of the moment as in pure iron, while the other two sites of Fe feel strongly the presence of the Cr neighbor that aligns a magnetic moment antiparallel to iron. For $x = 0.5$ ferromagnetic order is obtained as a result of a density of state effect in the $B2$ structure, while for the $B32$ structure

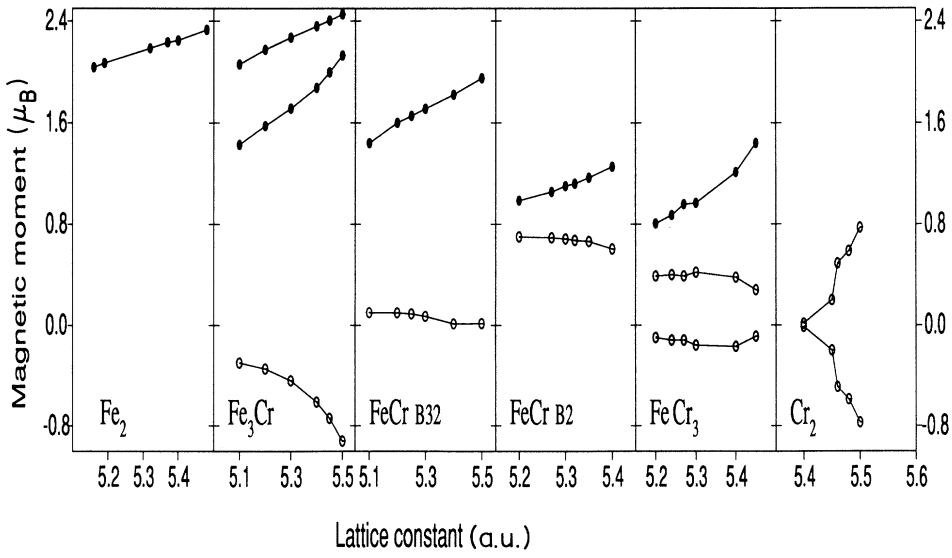

FIG. 4. Calculated local moments on Fe sites (full circles) and Cr sites (open circles) as a function of lattice constant for ordered Fe-Cr compounds .

Cr looses its moment and for other concentrations AF order is obtained. The FM ground-state in the B2 structure is understood from the NM electronic DOS, where a large peak in the DOS at E_f favors Stoner magnetism (Fig. 6). In ordered $FeCr_3$ compound we find a tendency to form an antiferromagnetic state. This concerns the Cr site, which is most distant from the Fe site, while the Cr adjacent to Fe are polarized FM and develop a larger moment. The magnetic Gruneisen parameter $\frac{\partial M}{\partial V}$ of local moment of iron for pure Fe, Fe_3Cr, FeCr, and $FeCr_3$ are 0.02, 0.04 (0.022), 0.031, and 0.057 ($\frac{\mu_B}{(a.u.)^3}$), respectively. The larger values near Invar compositions reflect the instability of magnetic moments. Our results show that nonequivalent Fe and Cr sites in the bcc structure have different magnetic properties, and short-range order therefore becomes important. The local moments on Fe and Cr sites and their s, p, d decomposition are reported in Table III. For a different environment the partial moments of s and p symmetry are aligned antiparallel to the $3d$ local moment.

Table III summarizes the results for the calculated hyperfine fields H_{hf} at the sites of Fe and Cr, while Fig. 5 shows the variation of H_{hf} versus the lattice parameter for the different FM ordered structure. H_{hf} is proportional to the electronic spin density at the nucleus. The main contribution to the core spin-density magnetization comes from the large negative values of the $2s$ electrons and from the positive values of $3s$ electrons. The values of H_{hf} follow in general the trends for the local moments as is known for pure elements. For pure Fe, the core s orbitals are polarized by the localized $3d$ spin density, to give a large negative spin density on the nucleus, which dominates the smaller spin density from the $4s$ valence. But the latter states hybridize with neighboring states and therefore give sensitive variations of H_{hf}. The precise proportionality between local moments and H_{hf} is lost, as is seen for Fe_3Cr at large volumes. Another observation is that different sites have quite different H_{hf} values, especially Cr sites. This is difficult to reconcile with the experimental findings [and of CPA (Ref. 47)], which show one continuous H_{hf} value for each element, varying with concentration. Again one is obliged to conclude that real materials consist of quite large domains of rather pure Fe or Cr composition, so that one H_{hf} value dominates the signal from each domain. However, some FeCr hybridization should exist, since the H_{hf} variations cannot be explained only from volume variations of the H_{hf} of the pure elements. In other words, the domains cannot be too large. This picture is consistent with that deduced from the total-energy results.

TABLE III. Magnetic properties of ordered Fe-Cr compounds. Here μ_s, μ_p, and μ_d are the partial spin moment, μ_{tot} is total moment (in μ_B units) for iron and cromium atom, and H_{hf} is the total hyperfine field at the nucleus. The $1s$, $2s$, and $3s$ orbital core hyperfine fields contributions (in kG units) are reported too. All the listed data are calculated at the equilibrium lattice constant except for Cr, where we have chosen a=5.45 a.u.

		Fe ($B2$)	Fe_3Cr ($D0_3$)		FeCr ($B2$)	FeCr ($B32$)	$FeCr_3$ ($D0_3$)
			Fe_1	Fe_2			
	s	−0.007	0.011	0.002	0.007	0.006	0.004
	p	−0.044	−0.015	−0.015	0.004	0.000	0.007
Fe	d	2.223	2.267	1.721	1.082	1.695	0.950
	Total	2.186	2.270	1.713	1.102	1.709	0.966
	H_{hf}	−320.5	−200.8	−188.	−82.9	−158.2	−91.3
	Total core	−300.8	−307.8	−232.6	−145.1	−229.4	−127.2
	$1s$	−21.6	−22.2	−17.1	−11.3	−17.3	−10.1
	$2s$	−608.5	−616.2	−471.2	−300.5	−463.4	−263
	$3s$	329.3	330.6	255.7	166.7	251.3	145.9

		Fe_3Cr ($D0_3$)	FeCr ($B2$)	FeCr ($B32$)	$FeCr_3$ ($D0_3$)		Cr ($B2$)
					Cr_1	Cr_2	
	s	−0.019	−0.003	−0.007	0.003	−0.001	0.002
	p	−0.045	−0.023	−0.010	−0.022	−0.066	0.000
Cr	d	−0.387	0.706	0.083	−0.164	0.427	0.179
	Total	−0.443	0.684	0.072	−0.158	0.420	0.178
	H_{hf}	−94.9	−105.8	−59.3	46.4	−57.8	−7.8
	Total core	52.2	−87.0	−9.5	21	−53.1	−22.7
	$1s$	2.9	−3.3	−0.6	1.2	−2.3	−0.9
	$2s$	67.5	−148.6	−21.8	31.4	−89.6	−35.6
	$3s$	−18.2	64.9	12.9	−11.6	38.8	13.8

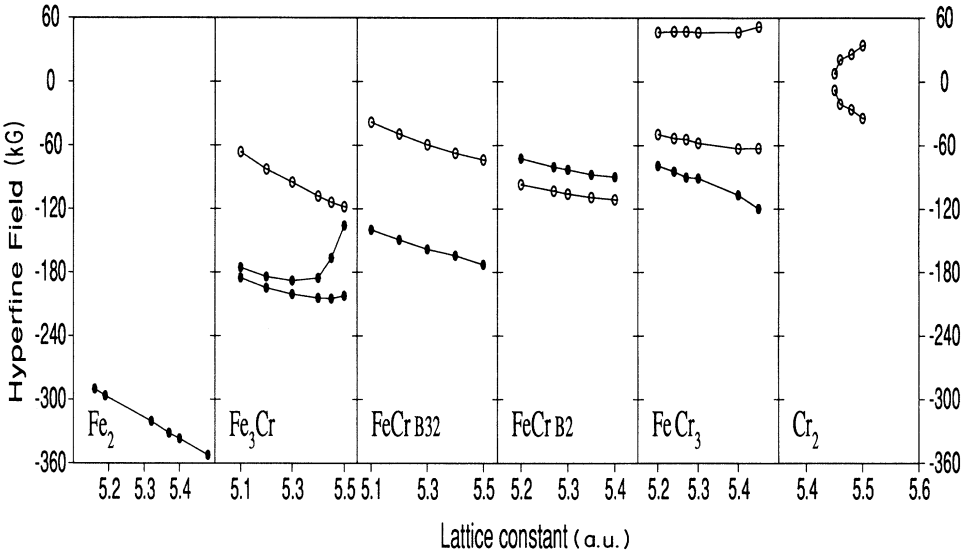

FIG. 5. Calculated hyperfine fields H_f on Fe sites (full circles) and Cr site (open circles) as a function of lattice constant for ordered Fe-Cr compounds .

B. Density of states and specific heat

The strong magnetism of certain ferromagnetic materials has been explained by Malozemoff, Williams, and Moruzzi[48] by the presence of the Fermi level in a minimum of the DOS of either the majority or minority spin. Similar predictions have been reported from rigid-band[10] theory although this theory is very simplified.

Our band-structure calculations of ordered NM Fe-Cr systems exhibit a constant number of d electrons on the Fe and Cr site. This constancy is valid only for the localized $3d$ electrons and not for s and p electrons, and has been reported for several other bcc Fe- and Co-based compounds.[48] In NM Fe-Cr the Fermi energy lies on the higher peak of Fe d DOS and on a minor peak or a valley of the Cr d DOS. There is an exception for $B2$ FeCr (unstable), where the Fermi level is positioned in the middle of a large peak not only of Fe but also of Cr. Figure 6 shows the partial DOS of Fe and Cr for ordered FeCr with $B2$- and $B32$-type structures and for a disordered bcc NM FeCr alloy. At this composition the shape of the DOS near the Fermi level is strongly related to local coordination.

In Fig. 7 are shown the spin-polarized partial DOS for Fe and Cr atoms for the studied FM ordered Fe-Cr compounds at their equilibrium lattice. Partial DOS of the same type of atoms of nonequivalent sites have been added together in order to visualize better the Fe and Cr contributions to the DOS. Qualitatively our calculated local DOS shows an increase of the number of states at the Fermi level when Cr is added. Not only the lattice but also the magnetic interactions and the local coordination influence strongly the shape of the DOS.

It has been observed that electronic specific heat $C_{\rm el}$ values are peaked near the Invar concentrations. This is the case for several fcc (FeNi, etc.) Invars as well as for bcc FeCr systems, and it is noted that this is not really an Invar effect, but is rather an effect associated with spin-glass behavior.[42] In the limit of low temperature, $C_{\rm el}(T) = \frac{\pi^2}{3}k^2TN(E_F)(1+\lambda_{\rm ep}+\lambda_s)$, where the λ's are enhancements due to electron-phonon coupling and spin fluctuations, respectively. The DOS at E_F, $N(E_F)$, is not particularly peaked in the Invar region. The lattice softening that occur due to the Invar effect is at large T and rather modest and cannot explain a drastic increase of $\lambda_{\rm ep}$. For the enhancement due to spins we can, in analogy with the calculation of $\lambda_{\rm ep}$, write $\lambda_s = N(E_F)I^2/K$ where I is a coupling matrix element and K is a "force constant" d^2E/dH^2, i.e., the second derivative of the total energy with respect to a magnetic field.[49] For paramagnetic materials K is large, since it costs a large energy to induce a change in magnetization. In an Invar system, the M and NM ground states are close in energy and it is easy to pass from one to another. The denominator K is small, making λ_s large, and we can qualitatively understand the enhancement of $C_{\rm el}$ as an effect due to the near degeneracy of M and NM states, as is one of the conditions for Invar behavior.

V. ELECTRONIC STRUCTURE IN DISORDERED $Fe_{1-x}Cr_x$ SOLID SOLUTION

A. Total energies of paramagnetic random alloys

For comparisons of total energies in the disordered case we discard those of magnetic calculations. The reason being that the magnetic moment of Cr is lost due to the assumption of complete disorder. In reality, different local environments allow for spatial fluctuations of the magnetic moments, favoring AF. Energies due to this and due to domain walls are not controlled in the approximation of complete disorder. However, we have calculated the electronic structure and the total energy of paramagnetic random solution using our self-consistent LES-LMTO method. For the stoichiometric compositions we use as starting potential the converged potential of the ordered supercell calculation. The disordered phases are

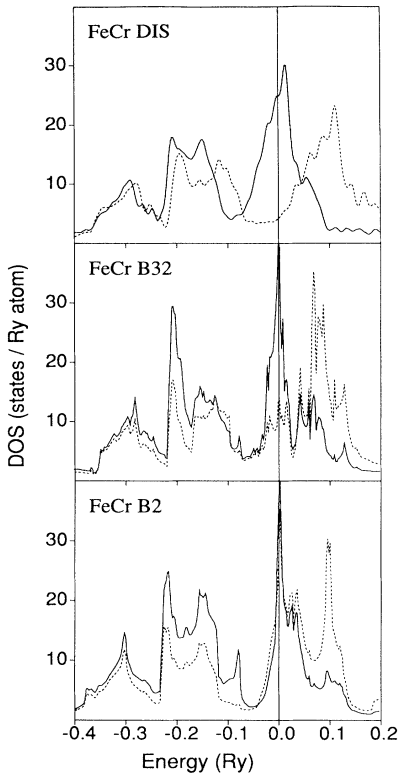

FIG. 6. Site-decomposed densities of states of Fe (solid line) and of Cr (dashed line) in ordered FeCr with $B32$ and $B2$ lattice type, and in disordered bcc FeCr. The lattice constant is 5.3 (a.u.)

found to be more stable than the ordered ones except near the Invar composition. The Madelung ordering energy for $FeCr_3$ and Fe_3Cr in the $D0_3$ structure is 7.4 and 8.1 mRy, respectively, while the Madelung ordering energy for FeCr in the $B2$ and $B32$ structure amounts to 14.5 and 2 mRy, respectively. The small Madelung energy of $B32$ reflects its stability over the $B2$ structure. In analogy with results obtained using the approximated CW method and the energy cluster expansion, the heat of mixing for the NM random solution calculated using our LES-LMTO method is positive. With respect to the NM-ordered structure we found that in the Cr-rich region the ordered phase is more stable than the disordered one, and the equilibrium lattice is shifted to higher values for the disordered phase. At zero temperature, the total energy variation as a function of lattice parameter is shown in Fig. 8 for NM $Fe_{25}Cr_{75}$ and $Fe_{50}Cr_{50}$. The disordered phases are compared with the respective ordered superstructure ($D0_3$ for $FeCr_3$, $B2$ and $B32$ for FeCr). The calculated equilibrium lattice constant, bulk moduli are, respectively, 5.28,5.34 (a.u.) and 3.3,2.75 Mbar for the $Fe_{50}Cr_{50}$ and $Fe_{25}Cr_{75}$ alloys. There is a very little shift to larger lattice equilibrium for the disordered phase; however, the accuracy of the total-energy calculation is lower than for the ordered supercell. We remind here that the total-energy calculations for random solid solution do not take into account the short-range order effects and therefore are less comparable to experimental findings.

B. Band-structure properties

In Table IV are reported the total and l-decomposed charges (in units of electron) of Fe and Cr for the different ordered structure and for the respective random solution. These results indicate that the total and partial charges are very similar in the ordered and disordered environment. Therefore, for NM system, the state of order plays no role for the charge properties and the charges scale with composition quite linearly. On the other hand, the band dispersions and Fermi-level properties can change drastically, and are related more to local coordination than to composition. The DOS for the $B32$ structure

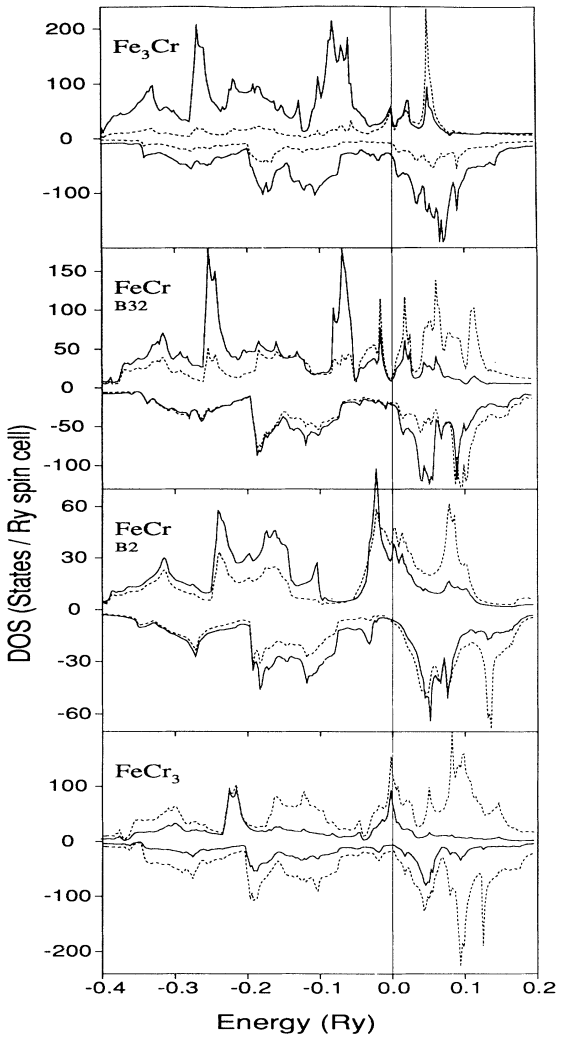

FIG. 7. Spin-polarized density of states in ordered FM Fe_3Cr, FeCr, $FeCr_3$ at their respective equilibrium minima. Site-decomposed densities of states of Fe are in solid line and for Cr are in dashed line.

TABLE IV. Calculated values of total charges Q_{ws} (in electrons) and partial charges decomposed in s-, p-, d-angular momentum components on Fe and Cr sites for all NM ordered and disordered Fe-Cr system. The charges are multiplied with the concentration in order to allow for a direct comparison between ordered and disordered cases.

State	Composition	Structure	Q_s	Q_p	Q_d	Q_{ws}	Q_s	Q_p	Q_d	Q_{ws}
				Fe				Cr		
	Cr_2	$B2$					0.61	0.79	4.53	6.00
	$FeCr_3$	$D0_3$	0.17	0.23	1.65	2.06	0.45	0.57	3.37	4.44
	FeCr	$B2$	0.34	0.42	3.30	4.10	0.29	0.36	2.21	2.90
ORD	FeCr	$B32$	0.33	0.43	3.28	4.08	0.29	0.36	2.23	2.92
	Fe_3Cr	$D0_3$	0.49	0.61	4.92	6.07	0.14	0.17	1.10	1.43
	Fe_2	$B2$	0.63	0.77	6.52	8.00				
	$Fe_{25}Cr_{75}$	bcc	0.15	0.16	1.69	2.01	0.46	0.60	3.38	4.49
DIS	$Fe_{50}Cr_{50}$	bcc	0.31	0.35	3.33	4.02	0.31	0.39	2.25	2.98
	$Fe_{75}Cr_{25}$	bcc	0.47	0.56	4.94	6.02	0.15	0.18	1.13	1.48

(Fig. 6) and for the disordered phase are very similar. The large peak of the DOS of Cr that is found at E_F in the $B2$ is shifted to larger energy in the $B32$ and in the disordered BCC environment, while the Fe DOS at E_F remains large in the three structures and is important for the magnetic stability. This indicates that the presence of the large peak of Cr at E_F in the $B2$ is really an effect due to ordering and that changing the number of neighbors or introducing some substitutional disorder affects strongly the electronic structure of Cr and much less the band dispersion of Fe. In agreement with these findings total-energy calculations show also that NM $B32$ phase is more stable than $B2$ and has an energy comparable to the energy of the disordered phase of FeCr (see Fig. 8).

The spin-resolved partial DOS projected on Fe and

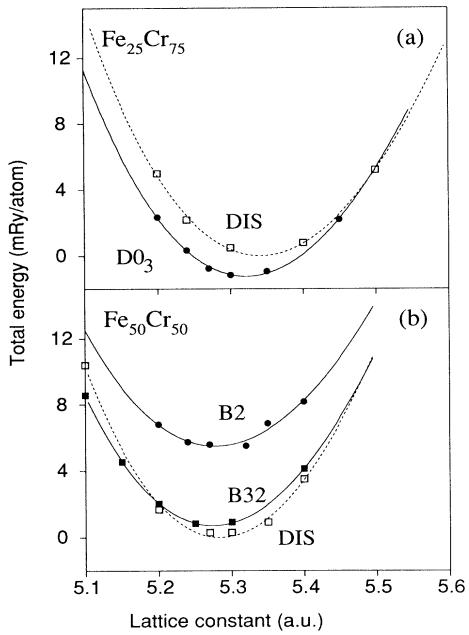

FIG. 8. (a) Total energies vs lattice constant for the NM state for ordered (full circles and solid line) $FeCr_3$ in the $D0_3$ structure and bcc disordered (open boxes and dashed line) $Fe_{75}Cr_{25}$. (b) Total energies vs lattice constant for the NM state for ordered FeCr in the $B2$ (full circle and solid line) and $B32$ structure (full boxes and solid line) and bcc disordered (open boxes and dashed line) $Fe_{50}Cr_{50}$.

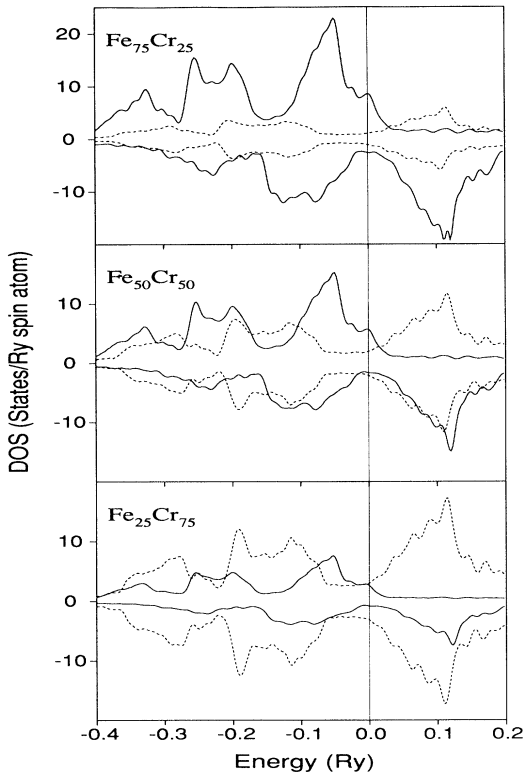

FIG. 9. Spin-resolved densities of states for disordered $Fe_{75}Cr_{25}$, $Fe_{50}Cr_{50}$, and $Fe_{25}Cr_{75}$ alloys. Site-decomposed densities of states of Fe are in solid line and for Cr are in dashed line.

Cr atoms are presented in Fig. 9 for disordered $Fe_{25}Cr_{75}$, $Fe_{50}Cr_{50}$ and $Fe_{75}Cr_{25}$. In agreement with previous CPA results,[11] our calculations indicate that the Fermi level is positioned in a valley between the bonding-antibonding minority spin DOS. This feature has proved to lead to an almost linear dependence of the average moment as a function of composition in the iron-rich region because electrons are added to the majority spin states without influencing the minority spin. A collapse of the magnetic moment occurs near the Invar region. Comparing at the same composition the projected DOS for the disordered alloys (Fig. 9) and for the respective ordered phases (Fig. 7) we see that near the Fermi energy all fine structures of the DOS (especially for Cr atoms) are washed out. For the disordered $Fe_{25}Cr_{75}$ alloy (in the Invar region) the large peak of Fe and Cr at the Fermi level present in the ordered structure is completely washed out, and this drastic reduction confirms the picture that the real material (characterized by a huge specific heat) is not a random solution but shows rather some orderered phase. Furthemore, the DOS shows that the splitting between the centers of the majority d bands of Fe and Cr are smaller than for the minority spin levels, indicating a localization of the majority electrons, while the minority states see a much stronger disorder. Similar effects are present in $Fe_{1-x}V_x$, in the $Fe_{1-x}Co_x$ system,[50] as well as in Invar $Fe_{65}Ni_{35}$.[51]

VI. CONCLUSION

We have presented a systematic investigations of the total energy and magnetic properties of $Fe_{1-x}Cr_x$ ordered and disordered alloys in the LSD approximation. The use of band-structure calculations for ordered and completely disordered systems, together with cluster expansion technique, have permitted a general study of M and NM properties of the Fe-Cr system. The results confirm two experimental findings. First, the calculations show that a high degree of segregation takes place in the Fe-Cr system, although one cannot directly indicate which type of clusters or domains are formed. Second, near the $Fe_{25}Cr_{75}$ compositions the total energy of M and NM configurations are almost degenerate and favorable for Invar properties. A direct comparison between experience and theory is not always possible because of the short-range order effects that are not taken into account in the theory. However, the comparison between completely disordered and ordered structure have permitted to analyze what properties are most sensitive to the change of order.

ACKNOWLEDGMENT

This work has been supported by the Swiss National Science Foundation under Grant No. 20-5446.87.

[1]V.E. Rode, S.A. Finkelberg, and A.I. Lyalin, J. Magn. Magn. Mater. **31-34**, 293 (1983).
[2]R.J.Weiss, Proc. Phys. Soc. **82**, 281 (1963).
[3]A.R. Williams, V.L. Moruzzi, C.D. Gelatt, J.Kubler, and K. Schwarz, J. Appl. Phys. **53**, 2019 (1980).
[4]A.T. Aldred, Phys. Rev. B **14**, 219 (1976); A.T. Aldred *et al., ibid.* **14**, 228 (1976).
[5]S.K. Burke and B.D. Rainford, J. Phys. F **13**, 441 (1983); **8**, L239 (1978).
[6]C.H. Cheng, C.T. Wei, and P.A. Beck, Phys. Rev. B **120**, 426 (1960).
[7]M. Furusaka, Y. Ishikawa, S. Yamaguchi, and Y. Fujino, J. Phys. Soc. Jpn. **55**, 2253 (1986).
[8]V.G. Rivlin and G.V. Raynor, Inter. Metals Rev. **1**, 21 (1980).
[9]D. Chandra and L.H. Schwartz, Metal. Trans. **2**, 511 (1971).
[10]H. Hasegawa and J. Kanamori, J. Phys. Soc. Jpn. **31**, 382 (1971)
[11]W.A. Shelton, Jr., F.J. Pinski, D.D. Johnson, D.M. Nicholson, and G.M. Stocks, in *Alloy Phase Stability and Design*, edited by G.M. Stocks, D.P. Pope, and A.F. Giamei, MRS Symposia Proceedings No. 186 (Materials Research Society, Pittsburgh, 1991).
[12]B. Drittler, N. Stefanou, S. Blugel, R. Zeller, and P.H. Dederichs, Phys. Rev. B **40**, 8203 (1989).
[13]M. Hennion, J. Phys. F **13**, 2351 (1983).
[14]O.K. Andersen, Phys. Rev. B **12**, 3060 (1975).
[15]T. Jarlborg and G. Arbman, J. Phys. F **7**, 1635 (1977).
[16]L. Hedin, B.I. Lundqvist, and S. Lundqvist, Solid State Commun. **9**, 537 (1971).
[17]O. Gunnarson and B.I. Lundqvist, Phys. Rev. B **13**, 4274 (1976).
[18]E.G. Moroni and T. Jarlborg, Phys. Rev. B **41**, 9600 (1990).
[19]F. Birch, J. Geophys. Res. **57**, 227 (1952); J. Appl. Phys. **9**, 279 (1938).
[20]J.W.D. Connolly and A.R. Williams, Phys. Rev. B **27**, 5169 (1983).
[21]R. Kikuchi, Phys. Rev. B **81**, 988 (1951).
[22]N.S. Golosov and A.M. Tolstick, J. Phys. Chem. Solids **36**, 899 (1975).
[23]L.G. Ferreira, A.A. Mbaye, and A. Zunger, Phys. Rev. B **35**, 6475 (1987).
[24]J.M. Sanchez, J.P. Stark, and V.L. Moruzzi, Phys. Rev. B **44**, 5411 (1991).
[25]E.G. Moroni and T. Jarlborg (unpublished).
[26]D.H. Seib and W.E. Spicer, Phys. Rev. B **2**, 1694 (1970).
[27]G.M. Stocks, R.W. Williams, and J.S. Faulkner, Phys. Rev. B **4**, 4390 (1971); H. Winter and G.M. Stocks, *ibid.* **27**, 882 (1983); J. Kudronovsky, V. Drchal, and J. Masek, *ibid.* **35**, 2847 (1987).
[28]B. Barbiellini, E.G. Moroni, and T. Jarlborg, J. Phys. Condens Matter **2**, 7597 (1990).
[29]G.L. Krasko and G.B. Olson, Phys. Rev. B **40**, 11536 (1989).
[30]D.J. Singh and J. Ashkenazi, Phys. Rev. B. **46**, 11570 (1992).
[31]H.J.F. Jansen and S.S. Peng, Phys. Rev. B **37**, 2689 (1988).
[32]C.S. Wang, B.M. Klein, and H. Krakauer, Phys. Rev. Lett. **54**, 1852 (1985).
[33]P. Bagno, O. Jepsen,, and O. Gunnarsson, Phys. Rev. B **40**, 1997 (1989).
[34]J.P. Perdew, Phys. Rev. Lett. **55**, 1655 (1985); J.P. Perdew and Y.Wang, Phys. Rev. B **33**, 8800 (1986).
[35]J.P. Perdew, Phys. Rev. B **33**, 8822 (1986); **34**, 7406 (1986).

[36]J. Kubler, J. Magn. Magn. Mater. **20**, 277 (1980).
[37]H.L. Skriver, J. Phys. F **11**, 97 (1981).
[38]J. Chen, D.J. Singh, and H. Krakauer, Phys. Rev. B **38**, 12 834 (1988).
[39]V.L. Moruzzi and P.M. Marcus, Phys. Rev. B **42**, 8361 (1990).
[40]E. Fawcett, Rev. Mod. Phys. **60**, 209 (1988).
[41]B. Barbiellini, E.G. Moroni, and T. Jarlborg, Helv. Phys. Acta **64**, 164 (1991).
[42]E.F. Wasserman, in *Ferromagnetic Materials*, edited by K.H.J. Bushow and E.P. Wohlfarth (North-Holland, Amsterdam, 1990), Vol. V, p. 240.
[43]E.G. Moroni and T. Jarlborg, in *Structure and Phase Stability of Alloys*, edited by J.L. Morán-López, F. Mejiá-Lira, and J.M. Sanchez (Plenum, New York, 1992), pp. 103–108.
[44]E.F. Wasserman, M. Acet, and W. Pepperhof, J. Magn. Magn. Mater. **90-91**, 126 (1990).
[45]M. Podgórny, Phys. Rev. B **45**, 797 (1992).
[46]A.E. Carlsson, Phys. Rev. B **35**, 4858 (1987).
[47]H. Ebert, H. Winter, D.D. Johnson, and F.J. Pinski, J. Phys. Condens. Matter **2**, 443 (1990).
[48]A.P. Malozemoff, A.R. Williams, and V.L. Moruzzi, Phys. Rev. B **29**, 1620 (1984).
[49]T. Jarlborg, Solid State Commun. **57**, 683 (1986).
[50]R. Richter and H. Eschrig, J. Phys. F **18**, 1813 (1988).
[51]D.D. Johnson, F.J. Pinski, and G.M. Stocks, J. Appl. Phys. **57**, 3018 (1985).
[52]S.H. Vosko, L. Wilk, and M. Nusair, Can. J. Phys. **58**, 1200 (1980).
[53]U. von Barth and L. Hedin, J. Phys. C **5**, 1692 (1972).
[54]H.J.F. Jansen, K.B. Hathaway, and A.J. Freeman, Phys. Rev. B **30**, 6177 (1984).
[55]D.J. Singh, W.E. Pickett, and H. Krakauer, Phys. Rev. B **43**, 11 628 (1991).